

October 19, 1995

**LOW ENERGY PARTICLE OSCILLATIONS AND CORRELATIONS WITH
HYDROMAGNETIC WAVES IN THE JOVIAN MAGNETOSPHERE:
ULYSSES MEASUREMENTS**

¹N. Krupp, ²H. Tsurutani, ³L.J. Lanzerotti and ³C.G. MacLennan

¹Applied Physics Laboratory / Johns Hopkins University, Laurel, MD 20723

²Jet Propulsion Laboratory, California Institute of Technology, Pasadena, CA 91109

³AT&T Bell Laboratories, Murray Hill, NJ 07974

ABSTRACT

We report on measurements of energetic particle modulations (ions and electrons with energies $E > 50$ keV) observed by the HI-SCALE instrument aboard the ULYSSES spacecraft that were associated with the only hydromagnetic wave event measured inside the Jovian magnetosphere by the ULYSSES magnetometer investigation. This wave event occurred during the high latitude, outbound pass of the spacecraft in the dusk sector of the planet at distances between 65 and 68 Jovian radii (R_J) and at southern magnetic latitudes between 27° and 32° . We show that the approximately five minute oscillations that occurred for about an hour in the north-south component of the magnetic field are well correlated with variations of the energetic particle fluxes at small pitch angles. The detection of the narrow angle ion beams by the HI-SCALE instrument occurs at the intersection between two angular spin sectors. The small amplitude waves vary the magnetic field direction sufficiently that the beam is directed primarily towards one sector and then the other, and back again. The plasma instability for wave generation is explained. We show that the waves are most likely to be generated by the presence of magnetospheric heavy ions (i.e. sulfur or oxygen) with energies in the range of a few keV.

INTRODUCTION

in February 1992 the ULYSSES spacecraft reached the planet Jupiter and remained inside the Jovian magnetosphere for almost 14 days (day 33-day 47 1992). The spacecraft entered the Jovian system in the morning sector (10:00 LT) similar to the other spacecraft Pioneer 10, 11 and Voyager 1, 2 that flew by the planet 1974 and 1979, respectively. However, on the outbound pass ULYSSES explored for the first time the dusk sector of the magnetosphere (around 18:00 LT) and departed the magnetosphere at high southern magnetic latitudes between 30 and 50° on its way out of the ecliptic plane to explore the southern pole of the Sun. Initial results of the encounter with Jupiter are published in *Science*, 257, 1992; *Planet. Space Science*, 41, 1993 and in *J. Geophys. Res.*, 98, 1993.

The Jovian magnetosphere was highly extended during the ULYSSES flyby. The first and last magnetopause crossings were observed at distances of 110 Jovian radii (R_J) on the inbound pass at 10:00 local time (LT) and 124 R_J on the outbound pass at 18:00 LT (Hammond et al., 1993; Phillips et al., 1993).

A power spectral analysis of the III-SCA II energetic particle data showed that unlike the magnetic field variations (which were essentially non-existent inside the Jovian magnetosphere during the ULYSSES encounter), the particle fluxes exhibit continuous variability over a wide frequency range (Lanzetta et al., 1993). Tsurutani et al. (1993) presented a survey of low frequency waves at Jupiter

during the ULYSSES encounter. In that paper, only one clear magnetospheric wave event was noted inside the magnetosphere for the entire encounter. It occurred during the outbound pass in the dusk sector of the planet at radial distances between 65 and 68 R_J and at southern magnetic latitudes between 27 and 32°. This wave event was observed at approximately half way between the closest approach at 6.31 R_J and the last magnetopause crossing. The magnetic field fluctuations last only one hour on day 42 of 1992, from 17:00 to 18:00 UT.

A detailed analysis of the energetic particle data from the HI-SCALE instrument during that time interval shows that variations were also observed in the measured particle intensities with the same periodicities. These combined observations suggest that ULYSSES observed wave particle interactions at high magnetic latitudes far away from the planet inside the Jovian magnetosphere. The observations presented in this paper therefore provide new insights into possible wave-particle interactions in a different region of the Jovian magnetosphere and extend the observations made by the Voyager spacecraft in the middle magnetosphere and at low magnetic latitudes (Khurana and Kivelson, 1989). The interaction mechanisms between particles and waves have been described theoretically i.e. by Gary et al. (1991); Thorne and Moses (1983); Thorne and Tsurutani (1987) and more generally in the series of papers by Southwood and Kivelson (1981, 1982); Kivelson and Southwood (1983, 1984) and earlier by Kennel and Petschek (1966).

Krupp et al.: Particle oscillations and waves in the Jovian magnetosphere

After a short description of the magnetometer and 11 I-S(A1.1) instruments on ULYSSES we present the correlations of the energetic particle intensities with the magnetic field measurements for that particular 1-hour interval, followed by a discussion of a possible explanation in terms of ion beam instabilities.

INSTRUMENT DESCRIPTIONS AND USED DATA SETS

(A) Magnetometer instrument

The magnetometer investigation on ULYSSES is composed of a vector helium magnetometer and a flux-gate magnetometer sitting on a boom far away from the spacecraft body. One magnetic vector per second is obtained from each sensor. The magnetometer instruments are described in detail in Balogh et al. (1992).

(B) HI-SCALE instrumentation

The HI-SCALE (Heliosphere Instrument for Spectra, Composition and Anisotropy at Low Energies) instrument on ULYSSES consists of 5 detector apertures in two separate telescope assemblies which form different angles with the spacecraft spin axis. HI-SCALE is able to measure electrons with energies between 40 and 300 keV in 4 different channels and ions ($Z \geq 1$) with energies between 50 and 5000 keV (assuming protons) in 8 different channels. The five detectors are identified as IEMS30, IEMS60, IEMS120, IEMS150 and CA60. The numbers in the names indicate the orientation of the telescopes central axes relative to the spin axis of the spacecraft. During each 12s-rotation the measured ions and electrons are sampled into 4 (IEMS30, IEMS150) and 8 sectors (IEMS120, IEMS60, CA60), respectively. With this design the HI-SCALE instrument provides measurements from 32 different directions in space every 12 seconds. We note that the HI-SCALE instrument cannot distinguish between ion species for energies < 0.5 MeV/nucleon and the detectors were not designed to

resolve the charge state of the measured ions in a multi-species plasma. However, the detector responses for single ion species are known from calibration. The energy responses for protons, oxygen and sulfur ions in the 8 energy channels of the LEFS30 and LEFS 120 ion detectors are summarized in Tables 1 and 2. More detailed information about the HI-SCALE instrument can be found in Lanzerotti et al. (1992a).

For this study we used 30-second averaged data sets from the magnetometer and the low energy HI-SCALE detectors LEFS30, LEFS60, LEFS 12.0 and LEFS 150.

As pointed out by Southwood and Kivelson (1981) the response of a particle detector in the presence of a wave is a strong function of particle energy and pitch angle. The HI-SCALE instrument is the first instrument which could provide quasi three-dimensional measurements with very high time resolution together with good pitch angle coverage and different energy channels inside the Jovian magnetosphere. Therefore it is an excellent instrument to study wave-particle phenomena,

OBSERVATIONS

Fig. 1 gives an overview of the trajectory of the ULYSSES spacecraft inside the Jovian magnetosphere in the Jovian Dipole system. Z_{m} indicates the distance from Jupiter's dipole axis which is tilted away from the rotation axis by 9.60° and ρ is the distance from the center of the planet. The arrow marks the period where the hydromagnetic wave event was observed: day 42., 17:00:18:00 UT, at 65-67 R_J and $27\text{-}32^\circ$ south magnetic latitude.

(A) Magnetometer observations

Fig. 2. shows the 1 sec. averaged magnetic field data for the 1-hour interval on day 42:17:00-18:00 UT, 1992. The upper three panels show the magnetic field components in the RTN-system. in the lower panel the total magnetic field is shown. A sinusoidal fluctuation in the N-component (which is approximately the north-south component) with a period of about 5 min. can clearly be seen. The other two components and the total magnetic field do not show this variation. A detailed analysis of the components, done by Tsurutani et al, (1993), showed that the amplitudes $\Delta B/B$ of the associated waves were on the order of 0.3. The waves were determined to be purely transverse to the magnetic field direction with little or no compressional components. They were left-hand elliptically to circularly polarized (in the spacecraft frame), propagating at angles between 100° and 43° to the magnetic field. As an example, Fig. 3a, b illustrates one cycle of the wave. at 17:22-17:27 UT. In this case the wave was

propagating at an angle of 210° relative to the magnetic field direction. The two hodograms B_x - B_y and B_x - B_z indicate that the wave was not plane polarized.

(B) HI-SCALE energetic particle observations

Fig. 4 shows 30 sec-averaged and sector averaged fluxes of electrons (165-300 keV) and ions (130-210 keV) for one day of data (day 42, 1992). The 1-hour time period where the wave event was observed is marked by the solid lines. The event occurred between two relative intensity maxima. Maxima in the particles were observed when the spacecraft was closer to the equatorial plasma sheet of the planet. This means that the wave event was observed when the plasma sheet was relatively distant from the spacecraft location but was moving towards the spacecraft. The particle data show clearly that large variations over a wide range of frequencies were observed in the fluxes.

The hour of the wave event is shown in more detail in Fig. 5a, b. Fig. 5a shows the fluxes of ions (61-77 keV) of the LEIS 120 detector for each sector separately on a linear scale. In two sectors (6 and 7) the measured fluxes were significantly higher than in the others. This was even more pronounced in the LEIS60 detector (electrons 42-65 keV), data for which is shown in Fig. 5b. In this figure one can clearly see a modulation of the fluxes in these two sectors 6 and 7 with a period of about 5 minutes. It also appears that the relative maxima of the modulations in sector 6 were anti-correlated to the maxima in sector 7.

In order to understand the directionality of the flux observations, the sector look directions of the low energy detector heads of the IHI-SCA1.1; instrument arc plotted in Fig. 6 on a unit sphere in the spacecraft system of reference. In this system the Z-axis (spin axis) always points towards Earth. During the Jupiter flyby the Y-axis was pointing south with respect to the ecliptic plane and the X-axis completes a right handed system. The arrow in the drawing marks the magnetic field vector with respect to the center of the sphere. From this figure it is clear that the sectors 6 and 7 of the IHI-S60 and IIMS 120 detectors were the sectors measuring particles along and against the magnetic field direction. Ions in sectors 6 and 7 of the IIMS120 detector were flowing along the magnetic field towards Jupiter. Electrons in sector 6 and 7 of IHI-S60 were flowing anti-field-aligned away from Jupiter. This counter streaming of ions and electrons, reported earlier by Lanzerotti et al. (1992b), is clearly seen in Fig. 7 where the cosine of the pitch angle is plotted against the normalized fluxes for electrons (upper panels) and ions (lower panels) for one energy channel as a function of time. These pitch angle distributions are typical for the entire hour where the hydromagnetic wave event was observed.

Fig. 8 shows the ratio of the fluxes in sectors 6 and 7 of the IHI-S60 detector (measuring electrons) and the IIMS 120 detector (measuring ions) together with the B_N -component of the magnetic field. The modulation of the particle fluxes is in phase with the directional change of the magnetic field independent of particle species or direction to the magnetic field. No phase shifts in opposite sectors along the, magnetic field were observed, Further analysis of the different energy channels of the IHI-

SCALB instrument showed that the modulation of the fluxes along the magnetic field was observed at all energies with the same amplitude on a logarithmic scale. As an example, the fluxes of 4 different electron energy channels measured in sector 6 of the 1.10360 detector arc shown in Fig. 9.

DISCUSSION

Observations of simultaneous particle and field modulations have been reported many times from measurements made inside the Earth's magnetosphere. In the case of the Earth, bounce- and drift resonant interactions have shown to be very important in modeling ULF wave interactions (Su et al., 1979; Su et al., 1980). In these discussions, the amplitude of the flux oscillations should grow as the resonance energy is approached, and phase shifts of particle fluxes in opposite sectors and between electrons and ions should be observed (Kremser et al., 1981). Neither an energy dependence nor any phase shifts in the sectorized particle fluxes were observed during the event presented here. We therefore will not discuss that particular wave-particle interaction.

From the observed magnetic field magnitude and the particle intensities we calculated the energy densities of the magnetic field $E_{\text{mag}} = B^2 / 2\mu_0$ and the particle energy densities E_i for the two extreme cases, assuming that the measured ions in the III-SCA II energy channels were 1) all protons or 2) all oxygen ions. In reality, the ions measured are a mixture of protons, helium and heavier ions (mostly oxygen and sulfur ions). The energy density E_i for species i is given by (Lanzerotti et al., 1980):

$$E_i = 4\pi \sum_{k=1}^8 \Delta E_k \frac{J_k(1) + J_k(4)}{2} \frac{E_k}{v_k}$$

where $[J_k(1) + J_k(4)]/2$ is the average flux of the sectors 1 and 4 perpendicular to the flow direction for ion energy channel k of the JEMS30 and JEMS20 detectors, ΔE_k is the energy channel width, and v_k and E_k are the velocity and energy of the ions in energy channel k . The results of this calculation are

shown in Fig. 10. The energy density of the magnetic field is seen to be larger than the particle energy densities by a factor of 2-4 assuming that all the counts are due to oxygen ions and about a factor of 10 higher assuming all protons are detected in the HI-SCAIB energy channels.

From this determination, it is clear that the \vec{B} -field was controlling the particles in the observed energy range. Whenever the magnetic field moved back and forth in the north-south direction the particles were forced to follow. The electrons flowing along the magnetic field were more tightly bound because of their smaller gyro radii. Thus, the wave-related oscillations are more pronounced in the electron channels.

To determine what particles could have generated the observed waves through plasma instabilities, we calculated the gyro frequencies Ω of electrons and ions in an average magnetic field of 9 nT and compared them with the frequencies of the observed waves $\omega = 2\pi / T = 0.02$ Hz as listed in Table 3. The gyro frequencies of the heavy ions are seen to be comparable to the frequencies of the waves. The electron gyro frequency, however, was larger by 4 orders of magnitude.

The ion cyclotron resonance energy can be calculated under the usual assumption of doppler-shifted cyclotron resonance where the \vec{k} -vectors of the observed waves and the velocity vector \vec{v} of the ions are anti-parallel. The resonance condition is given by

$$\begin{aligned}\omega - \vec{k} \cdot \vec{v} &= \Omega_i \\ \omega + k_{\parallel} v_{\parallel} &= \Omega_i\end{aligned}$$

where only the parallel components were taken into account. If we then take the Alfvén velocity \vec{v}_A as the phase velocity ω/k_{\parallel} of the waves, we get the parallel velocity along the magnetic field

$$\vec{v}_{\parallel} = \vec{v}_A \left(\frac{\Omega_i}{\omega} - 1 \right)$$

The Alfvén velocity \vec{v}_A in Table 4 was calculated by using the electron plasma density $N_{\text{plasma}} = 0.03 \text{ cm}^{-3}$, reported for that interval by Bame et al. (1992).

The resonant energy for protons in this determination is above the measurable energy range of the HI-SCAIFI instrument and the resonant energies for the heavier ions are lower. For singly-charged oxygen and sulfur, for example, the resonant energies are 12 and 1 keV, respectively. Although these energies are lower than the HI-SCAIFI detector thresholds, the ion beam densities can be calculated from the measured differential flux $j_i(E_i)$ in the sectors along the magnetic field (Krimigis et al., 1981):

$$N_i = \int_0^{4\pi} d\Omega \int_0^{\infty} j_i(E_i) \frac{dE_i}{v_i}$$

where v_i is the ion velocity. For a particle detector with a limited energy range we find

$$N_i \approx 4\pi \sum_{k=1}^8 \left[\Delta E_i \frac{j_i(E_i)}{v_i} \right]_k$$

where k is the number of the energy channel, and ΔE_i is the energy channel width for species i . Taking all 8 energy channels into account, we calculated the 1-hour time averaged ion beam densities assuming

protons and oxygen ions; this is summarized in Table 5. We find that an oxygen beam would have had a density of 1.9% of the ambient plasma density, which is more than 3 times higher than the density of a proton beam (0.6% of the plasma density).

From the fact that field aligned ion beams were observed and from the observations that the waves were purely transverse and left-handed polarized, we can assume that the most likely wave-particle interaction for that hydromagnetic wave event is the ion-beam-instability. Gary et al. (1984, 1985) and also Gary (1991) provide the conditions for the maximum wave growth rates for resonant and non-resonant ion beam instabilities are given. In these papers it is shown that in the case of non-resonant interactions a positive growth rate of the waves is only possible if the beam velocity exceeds the Alfvén speed by a factor of 10. This case can be ruled out for the presented event because the maximum ion beam velocity for heavier ions was only 1-4 times the Alfvén speed (see Table 4). Following these arguments the most probable wave-particle interaction during that hydromagnetic wave event was the resonant ion beam instability. The most probable ion candidates were 12-106 keV oxygen ions or 1-12 keV sulfur ions.

SUMMARY

1. We have observed waves with approximately 5 minute periods inside the Jovian magnetosphere in the dusk sector of the plane at radial distances between 65 and 67 R_J and at high southern magnetic latitudes between 2.7° and 32° .
2. The waves were associated with flux oscillations in energetic particles ($E > 50$ keV) measured by the III-SCALE instrument at small pitch angles.
3. The resonant ion beam instability of 12-106 keV oxygen or 1-12 keV sulfur ions was the most probable wave-particle interaction.

ACKNOWLEDGMENTS

We are grateful to all the III-SCALÉ team members and especially acknowledge the work in III-SCALÉ data reduction at the University of Kansas by D. Haggerty and T.P. Armstrong and the extensive work in providing a powerful software package from S.J. Tappin at the University of Birmingham, UK. We thank S.F. Hawkins III (JHU/APL) in evaluating Fig. 10. Special thanks to A. Buttigieg (Observatoire de Meudon, France) for sharing the software to draw Fig. 6. Portions of this work were performed at the Jet Propulsion Laboratory, California Institute of Technology under contract with NASA. The work at JHU/APL and at AT&T Bell Labs. were also done under contract with NASA.

REFERENCES

Balogh, A., T.J. Beck, R.J. Forsyth, P.C. Hedgecock, R.J. Marquedant, E.J. Smith, D.J. Southwood and B.T. Tsurutani, The magnetic field investigation on the Ulysses mission: Instrumentation and preliminary results, *Astron. Astrophys. Suppl. Ser.*, 92,221, 1992.

Bame, S. J., B.L. Barraclough, W.C. Feldman, G.R. Gisler, J.T. Gosling, D.J. McComas, J.J. Phillips, M.F. Thomsen, B.E. Goldstein and M. Neugebauer, Jupiter's Magnetosphere: Plasma description from the Ulysses flyby, *Science*, 257, 1539-1543, 1992.

Gary, S.P., C.W. Smith, M.A. Lee, M. L. Goldstein and D. W. Forslund, Electromagnetic ion beam instabilities, *Phys. Fluids*, 27, 1852-1862, 1984.

Gary S.P., C.D. Madland and B.T. Tsurutani, Electromagnetic ion beam instabilities: II, *Phys. Fluids*, 28,3691-3695, 1985.

Gary, S. P., Electromagnetic ion/ion instabilities and their consequences in space plasmas: A review, *Space Sci. Rev.*, 56,373-415, 1991.

Hammond C. M., J.J. Phillips, S.J. Bame, F.J. Smith and C.G. MacLennan, Ulysses observations of the planetary depletion layer at Jupiter, *Planet. Space Sci.*, 41, 857-868, 1993.

Kennel C.F. and H.E. Petschek, Limits on stably trapped fluxes, *J. Geophys. Res.*, **71**, 1, 1966.

Khurana K.K. and M.G. Kivelson, Ultralow Frequency MHD Waves in Jupiter's Middle Magnetosphere, *J. Geophys. Res.*, 94, 5241-5254, 1989.

Kivelson M.G. and D.J. Southwood, Charged Particle Behavior in Low-Frequency Geomagnetic Pulsations, 3. Spin Phase Dependence, *J. Geophys. Res.*, **88**, 174-182, 1983.

Kivelson M.G. and D.J. Southwood, Charged Particle Behavior in Low-Frequency Geomagnetic Pulsations, 4. Compressional Waves, *J. Geophys. Res.*, 89, 1486-1498, 1984.

Kremser, G., A. Korth, J.A. Fejer and B. Wilken, Observations of Quasi-Periodic Flux Variations of Energetic Ions and Electrons With Pc 5 Geomagnetic Pulsations, *J. Geophys. Res.*, 86, 3345-3356, 1981.

Krimigis, S. M., J.F. Carbary, E.P. Keath, C.O. Bostrom, W.J. Axford, G. Gloeckler, L.J. Lanzerotti and T.P. Armstrong, Characteristics of Hot Plasma in the Jovian Magnetosphere: Results From the Voyager Spacecraft, *J. Geophys. Res.*, 86, 8227-8257, 1981.

Lanzerotti L.J., C.G. MacLennan, S.M. Krimigis, T.P. Armstrong, K. Behannon and N.F. Ness, Statics of the nightside Jovian plasma sheet, *Geophys. Res. Lett.*, 7, 817-820, 1980.

Lanzerotti L. J., R.E. Gold, K.A. Anderson, T.P. Armstrong, R.P. Lin, S.M. Krimigis, M. Pick, E.C. Roelof, E.T. Sarris, G.M. Simnett and W.F. Irwin, Heliosphere instrument for spectra, composition and anisotropy at low energies, *Astron. Astrophys. Suppl. Ser.*, 92, 349-363, 1992a,

Lanzerotti, L. J., T.P. Armstrong, R.E. Gold, K.A. Anderson, S.M. Krimigis, R.P. Lin, M. Pick, E.C. Roelof, E.T. Sarris, G.M. Simnett, C.G. MacLennan, H.I.P. Choo and S.J. Tappin, The hot Plasma Environment at Jupiter: An Overview of the Ulysses Encounter, *Science*, 257, 1518, 1992b.

Lanzerotti, L. J., T.P. Armstrong, C.G. MacLennan, G.M. Simnett, A.F. Cheng, R.E. Gold, D.J. Thomson, S.M. Krimigis, K.A. Anderson, S.E. Hawkins III, M. Pick, E.C. Roelof, E.T. Sarris and S.J. Tappin, Measurements of hot plasmas in the magnetosphere of Jupiter, *Planet. Space Sci.*, 41, 893-917, 1993.

Phillips J.] . . . S.J. Bamc, B.L. Barraclough, D.J. McComas, R.J. Forsyth, P. Canu and P.J. Kellogg, Ulysses plasma electron observations in the Jovian magnetosphere, *Planet. Space Sci.*, 41, 877-892, 1993.

Southwood, D.J. and M.G. Kivelson, Charged Particle Behavior in Low-Frequency Geomagnetic Pulsations, 1. Transverse Waves, *J. Geophys. Res.*, 86, 5643-5655, 1981.

Southwood, D.J. and M.G. Kivelson, Charged Particle Behavior in Low-Frequency Geomagnetic Pulsations, 2. Graphical Approach, *J. Geophys. Res.*, 87, 1707-1710, 1982.

Su, S.-Y., A. Konradi, T.A. Fritz, On Energy Dependent Modulation of the ULF Ion Flux Oscillations Observed at small Pitch Angles, *J. Geophys. Res.*, 84, 6510-6516, 1979.

Su, S.-Y., R.J. McPherron, A. Konradi, T.A. Fritz, Observations of ULF Oscillations in the Ion Fluxes at Small Pitch Angles with ATS 6, *J. Geophys. Res.*, 85, 515-522, 1980.

Thorne R.M. and J. Moses, Electromagnetic ion-cyclotron Instability in the Multi-ion Jovian Magnetosphere, *Geophys. Res. Lett.*, 10, 631-634, 1983.

Thorne R.M. and B.T. Tsurutani, Resonant interaction between cometary ions and low frequency electromagnetic waves, *Planet. Space Science*, **35**, 1501, 1987.

Tsurutani B.T., D.J. Southwood, Edward J. Smith and A. Balogh, A survey of low frequency waves at Jupiter: Ulysses encounter, *J. Geophys. Res.*, 98, 21203-21216, 1993.

I	JEMS30	proton response [keV]	oxygen response [keV]	Oxygen response [keV/nucleon]	sulfur response [keV]	sulfur response [keV/nucleon]
P1	56-78	(128-160)	(8-10)	(<384)	(<12)	
P2	78-130	(160-256)	(10-16)	(<384)	(<12)	
P3	130-210	256-384	16-24	(<384)	(<12)	
P4	210-340	384-744	24-34	512-640	16-20	
P5	340-600	544-880	34-55	640-960	20-30	
P6	600-1100	880-1440	55-91	960-1632	30-51	
P7	1100-1800	1456-2240	91-140	1632-2624	51-82	
P8	1800-4750	2240-160000	140-10000	2.624-457600	82-14300	

Table 1: Energy responses for protons, oxygen- and sulfur ions of the III-SCALE JEMS30 ion detector (adapted from Lanzerotti et al., 1993). The values in brackets are extrapolated.

LEMS120	proton response [keV]	oxygen response. [keV]	oxygen response [keV/nucleon]	sulfur response [keV]	sulfur response [keV/nucleon]
P1'	61-77	(128-160)	(8-10)	(<384)	(<12)
P2'	77-130	(160-256)	(10-16)	(<384)	(<12)
P3'	130-210	256-368	16-23	(<384)	(<12)
P4'	210-340	368-544	23-34	448-640	14-20
P5'	340-600	544-880	34-55	640-1088	20-34
P6'	600-1120	880-1520	55-95	1088-1632	34-51
P7'	1120-1870	1520-2400	95-150	1632-2752	51-86
P8'	1870-4800	2400-16000	150-1000	2752-457600	86-14300

Table 2: Energy responses for protons, oxygen- and sulfur ions of the HI-SCALE LEMS 120 ion detector (adapted from Lanzerotti et al., 1993). The values in brackets are extrapolated.

particle	charge [e]	Ω_i [Hz]
p	1	0.87
O^+	1	0.05
O^{2+}	2	0.11
S^+	1	0.03
S^{2+}	2	0.05
S^{3+}	3	0.08
e^-		1591

Table 3: Gyro frequencies of different particles and charges in a 9 nT magnetic field

ion	v_A [km/s]	v_{\parallel} [km/s]	E_{\parallel} [keV]	E_{\parallel} [keV/N]
p	1008	42500	9374	9374
O⁺	2.52	378	11.86	0.74
O²⁺	252	1131	106.78	6.67
S⁺	178	89	1.32	0.04
S²⁺	178	267	11.84	0.37
S³⁺	178	534	47.35	1.48

Table 4: Alfvén velocity v_A , derived velocities along the magnetic field v_{\parallel} and resonance energies E_{\parallel} of different ions.

particles (energy range)	avg. ion beam density $N_{\text{beam}} [\text{cm}^{-3}]$
protons (61-4800 keV)	1.99×10^4
oxygen ions (125-160000 keV)	5.71×10^4

Table 5: Calculated averaged ion beam densities during the observed hydromagnetic wave event inside the Jovian magnetosphere for the 1-hour interval of day 4217:00-18:00 in 1992.

FIGURE CAPTIONS

Fig. 1

Ulysses trajectory in magnetic coordinates.

Fig. 2

Ulysses high resolution magnetic field components and total magnetic field for 1992, day 42, 17:00-18:00 UT in the RTN-coordinate system

Fig. 3

(a) Bx-By-Hodogram in the spacecraft frame (S/C) for one wave cycle 1992, day 42., 17:22-17:27 UT

(b) Bx-Bz-Hodogram in the spacecraft frame (S/C) for one wave cycle 1992, day 42, 17:22-17:27 UT

Fig. 4

Ulysses HI-SCALE ion (130-210 keV) and electron (175-315 keV) fluxes for 1992, day 42

Fig. 5

(a) Ulysses HI-SCALE ion fluxes (61-77 keV) for angular spin sectors 1-8 of the IEFMS 120 detector

(b) Ulysses HI-SCALE electron fluxes (42-65 keV) for angular spin sectors 1-8 of the IEFMS60 detector

Fig. 6

Sector look directions (1-8) of the 1.1 IMS30, LBS60, LBS120, and the LBS150 detectors of the 11 I-SCAIB instrument, projected on the surface of a unit sphere. X, Y, and Z represent the S/C-system where the Z-axis points towards Earth. \mathbf{B} indicates the magnetic field vector relative to the center of the unit sphere during the event presented in the paper.

Fig. 7

Normalized differential fluxes versus the cosine of the pitch angle for electrons (upper panels) and ions (lower panels) as a function of time from left to right.

Fig. 8

Ratio of the fluxes in sector 6 and 7 for 61-77 keV ions (dashed) and 42-65 keV electrons (dotted) compared with the modulation in the north-south component of the magnetic field B_N (solid) during the hour of the event.

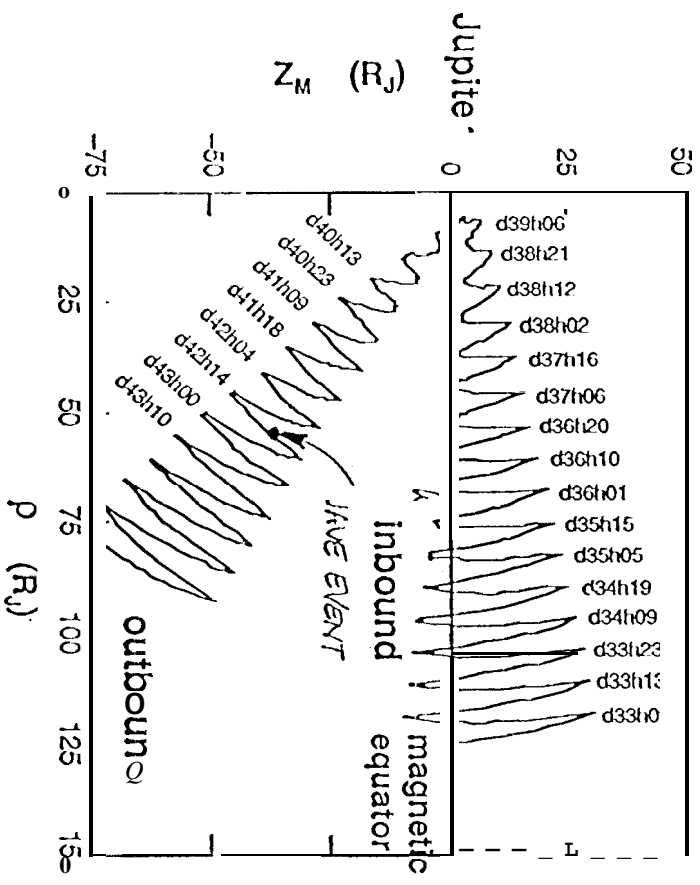
Fig. 9

Electron fluxes in sector 6 in 4 different energy channels (42-290 keV) during the event.

Fig. 10

Calculated energy densities for protons (56-4800 keV), oxygen ions (8- 10000 keV/nucleon) compared to the magnetic energy density.

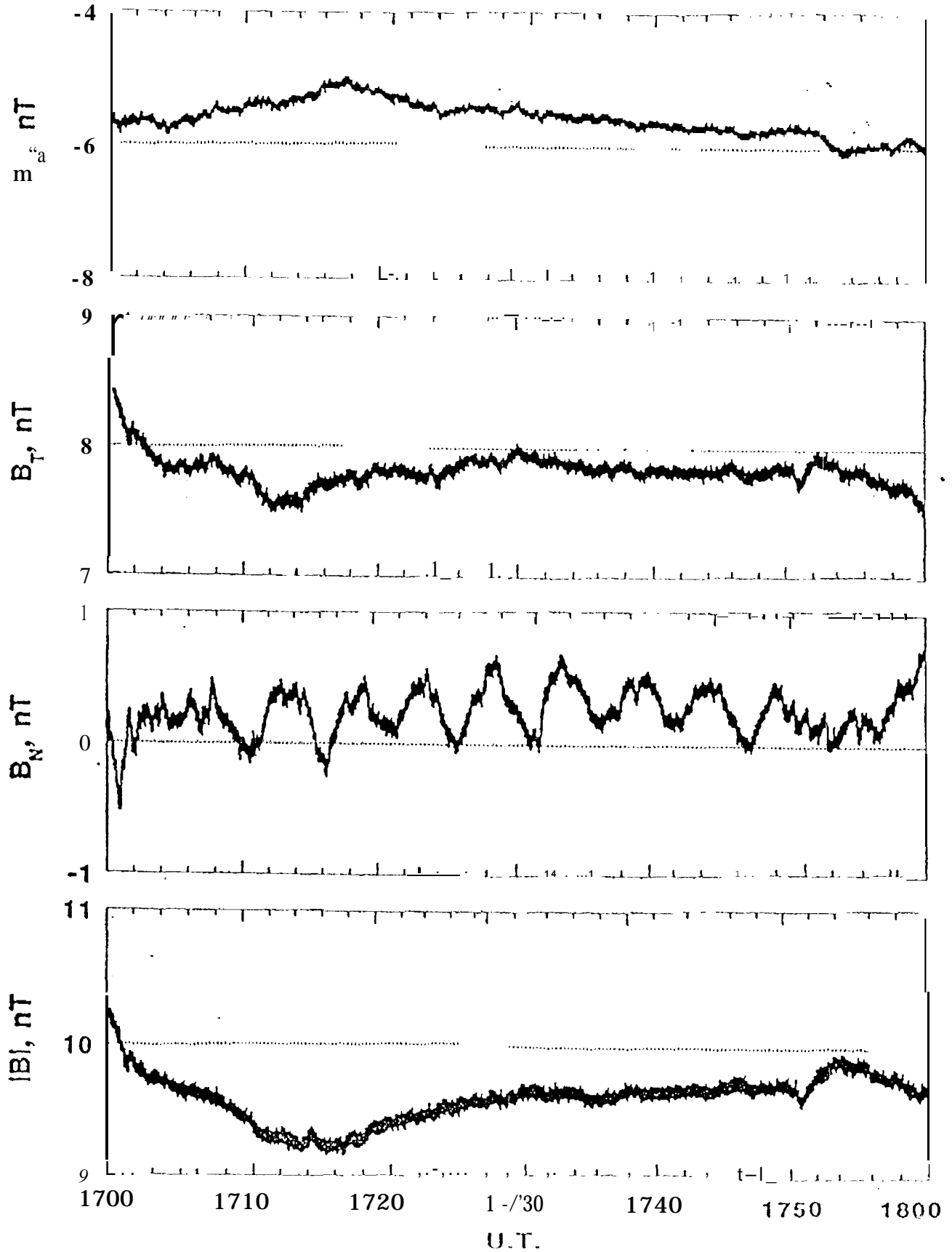
ULYSSES trajectory in magnetic coordinates



Ulysses VHMbig} resolution
SH Coordinates

February 11, 1992
Day 042

FIG. 2



ULYSSES Bx-By-Hodogram
Jupiter 92.042 17:22-17:27 UT

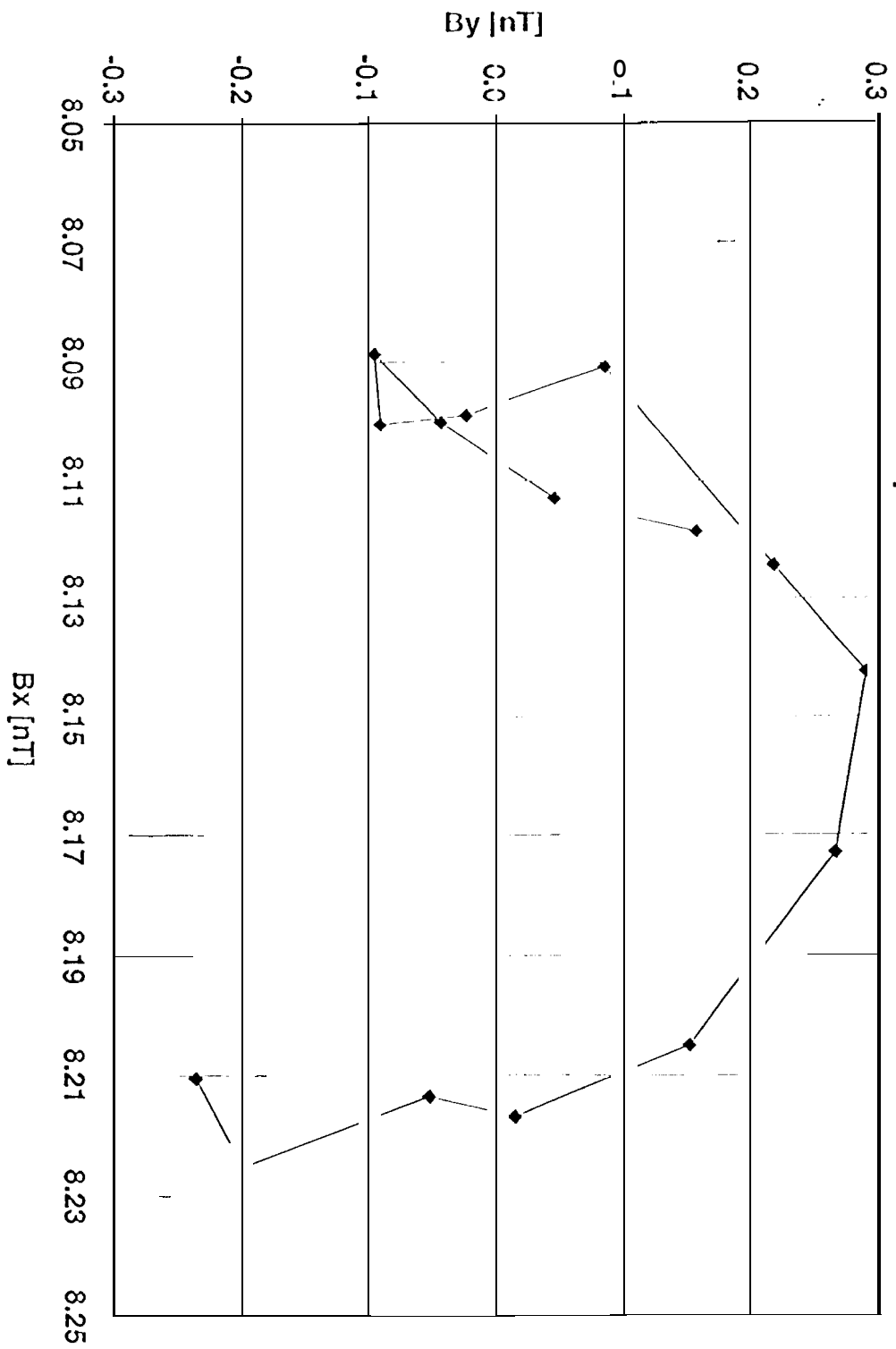
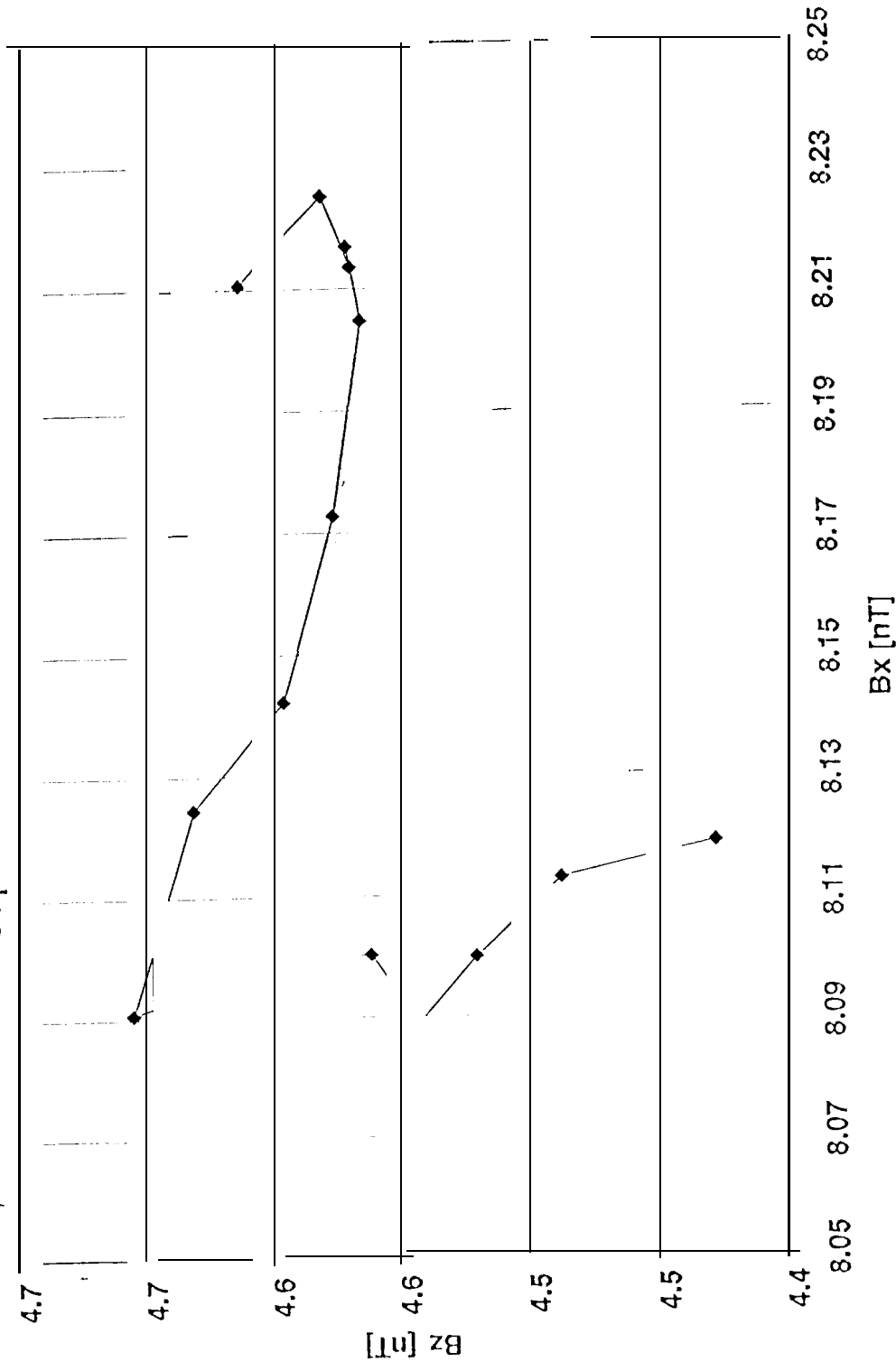


FIG. 3b.

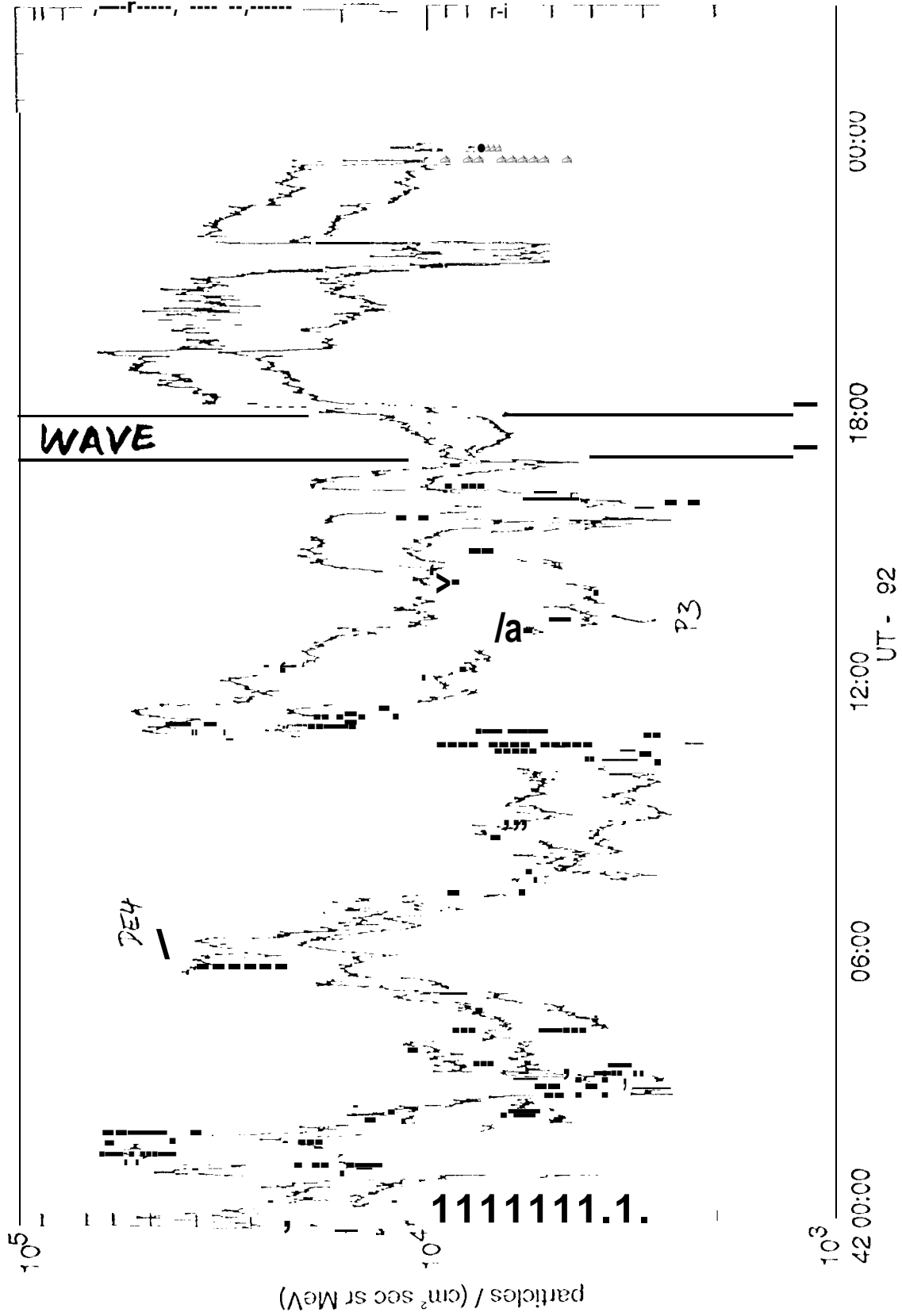
ULYSSES Bx-Bz-Hodogram
Jupiter 92.042 17:22-17:27 UT



F U X OI: P3, UE4
Sectors averaged, Averaged at 30.0s

HS V3.05 © Thu Jun 29 15:51:31 1985 by krupp

Source - 111a02040.3 14 . OF = 5 03



P3 140-710 1601 1.1.0
UE4 140-5501 1601 1.1.0

Fig 5a

ULYSSES HI-SCALE

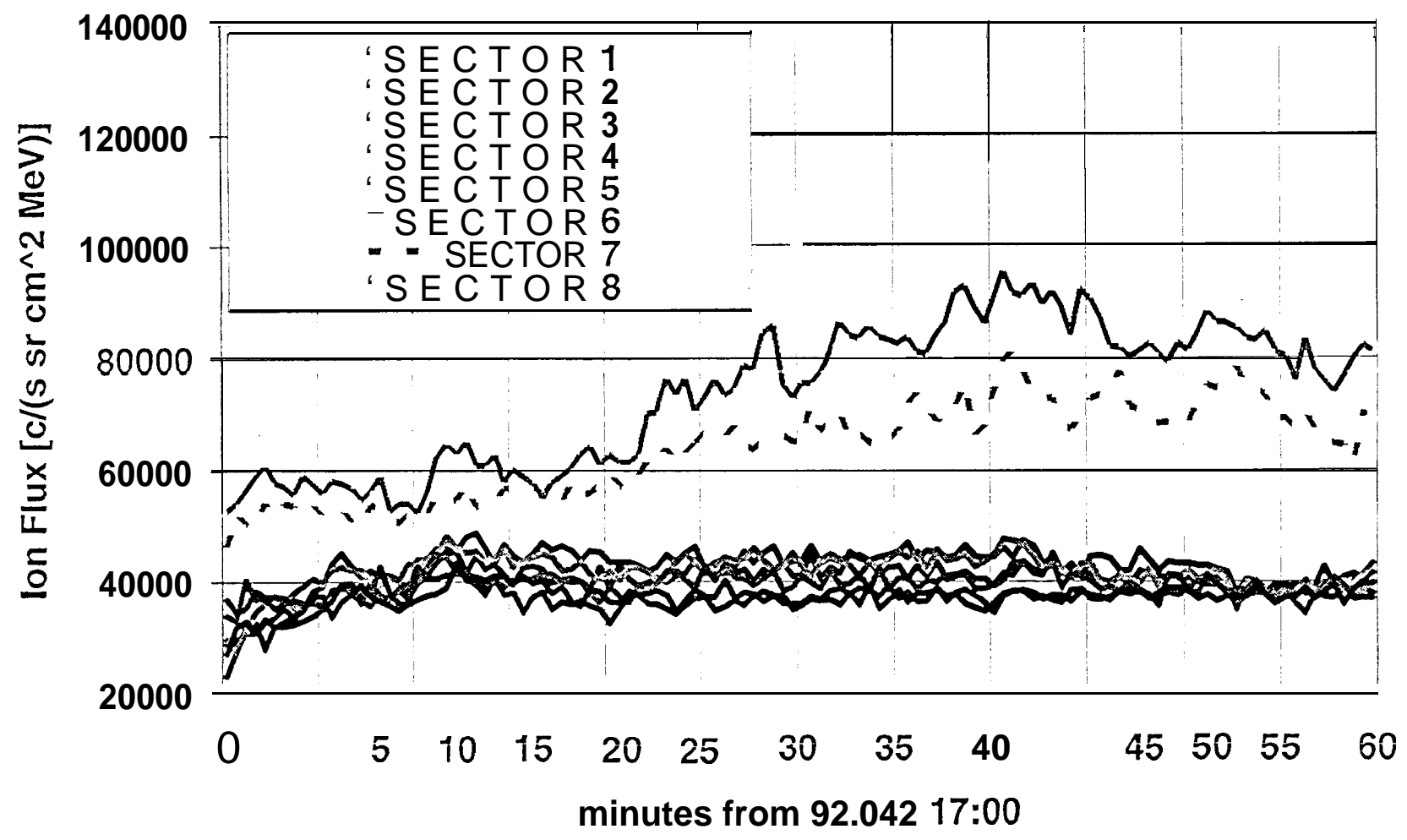


FIG 5b
11/1/84

ULYSSES HI-SCALE LEFS60 E1' (42-65 keV)

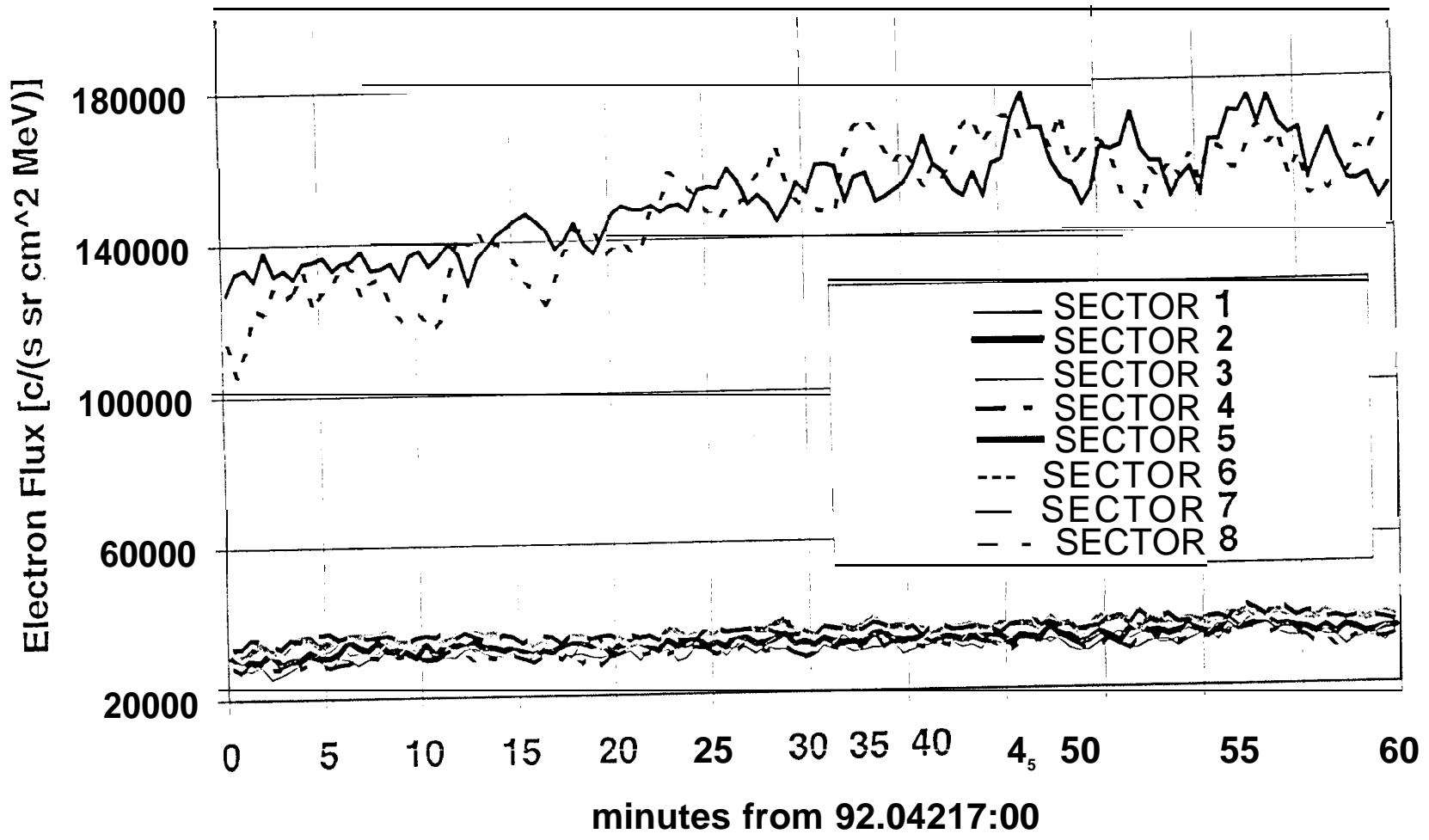
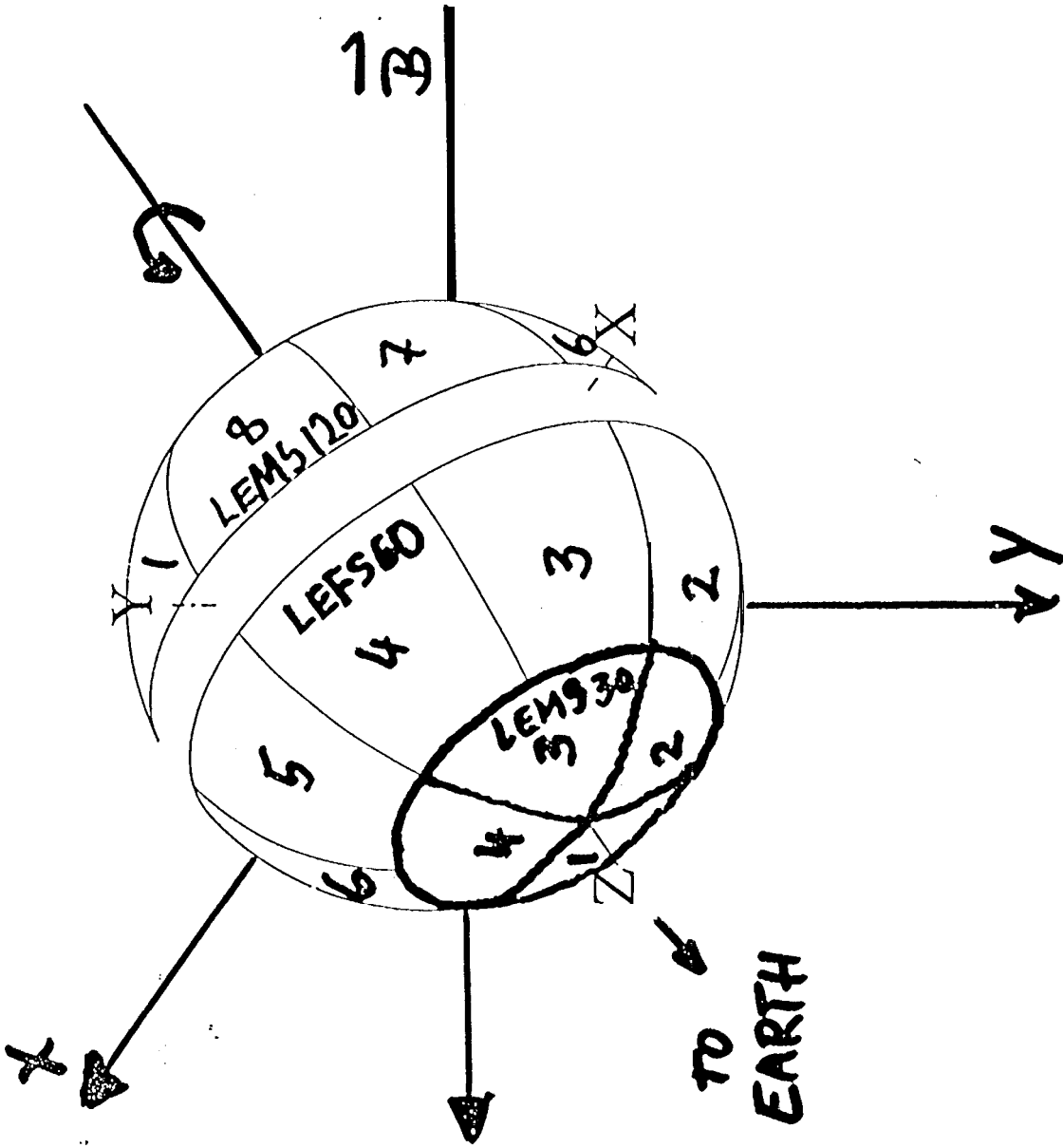
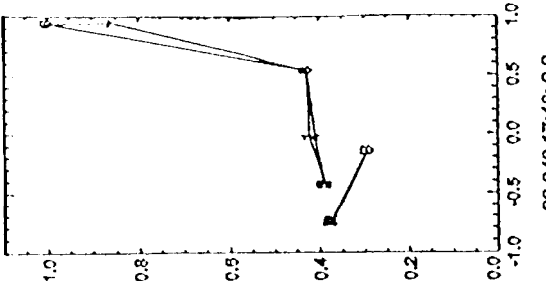
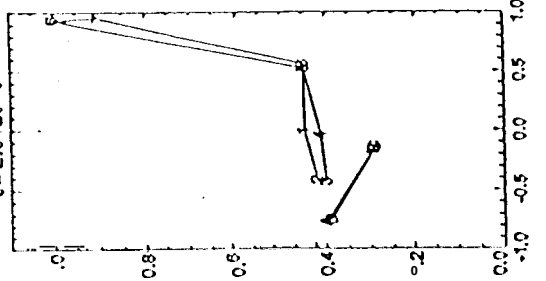
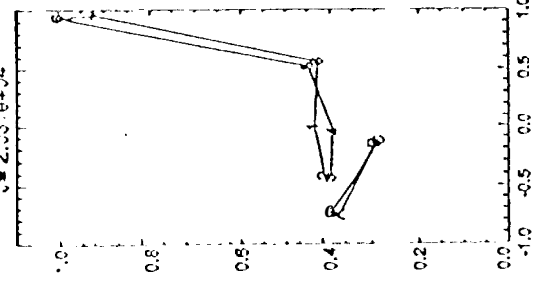
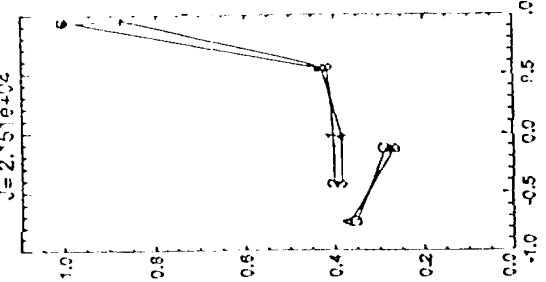
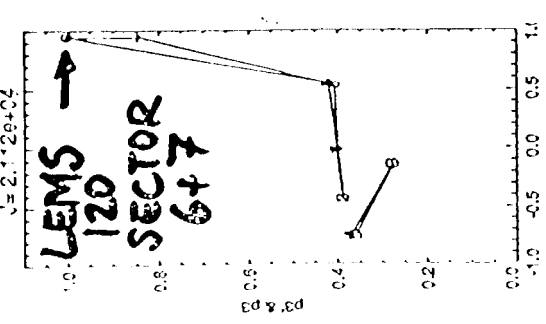
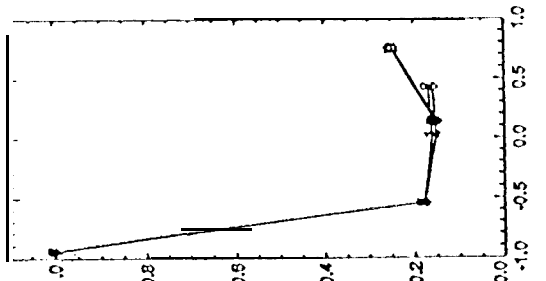
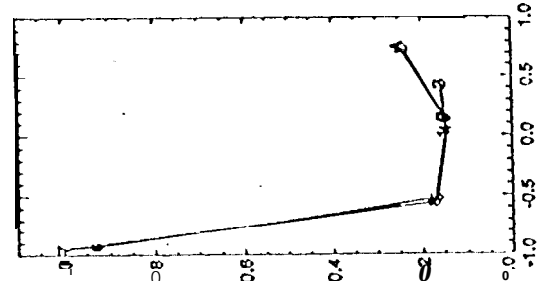
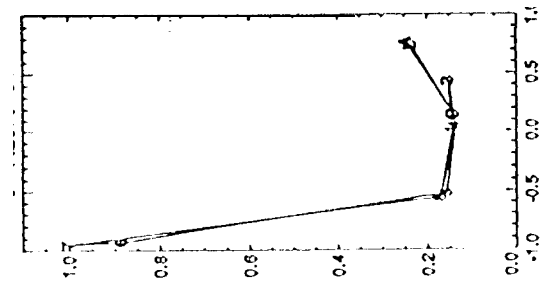
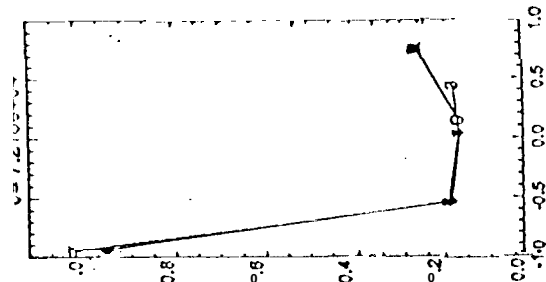
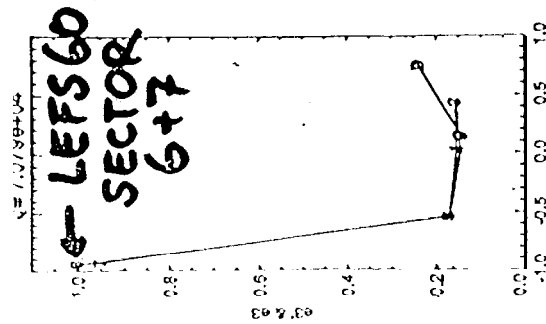


FIG. 6



Normalized differential u_1 vs $\cos \mu$ ang.e/
 Averaged over ± 1.00 m

HS V3.05 @Thu Apr 20 11:01:05 1995 by krupp



92 042 17:44:0.0
 92 042 17:45:0.0
 (59.2, -0.5)

92 042 17:45:0.0
 92 042 17:46:0.0
 (59.2, 0.5)

92 042 17:46:0.0
 92 042 17:47:0.0
 (58.9, 1.7)

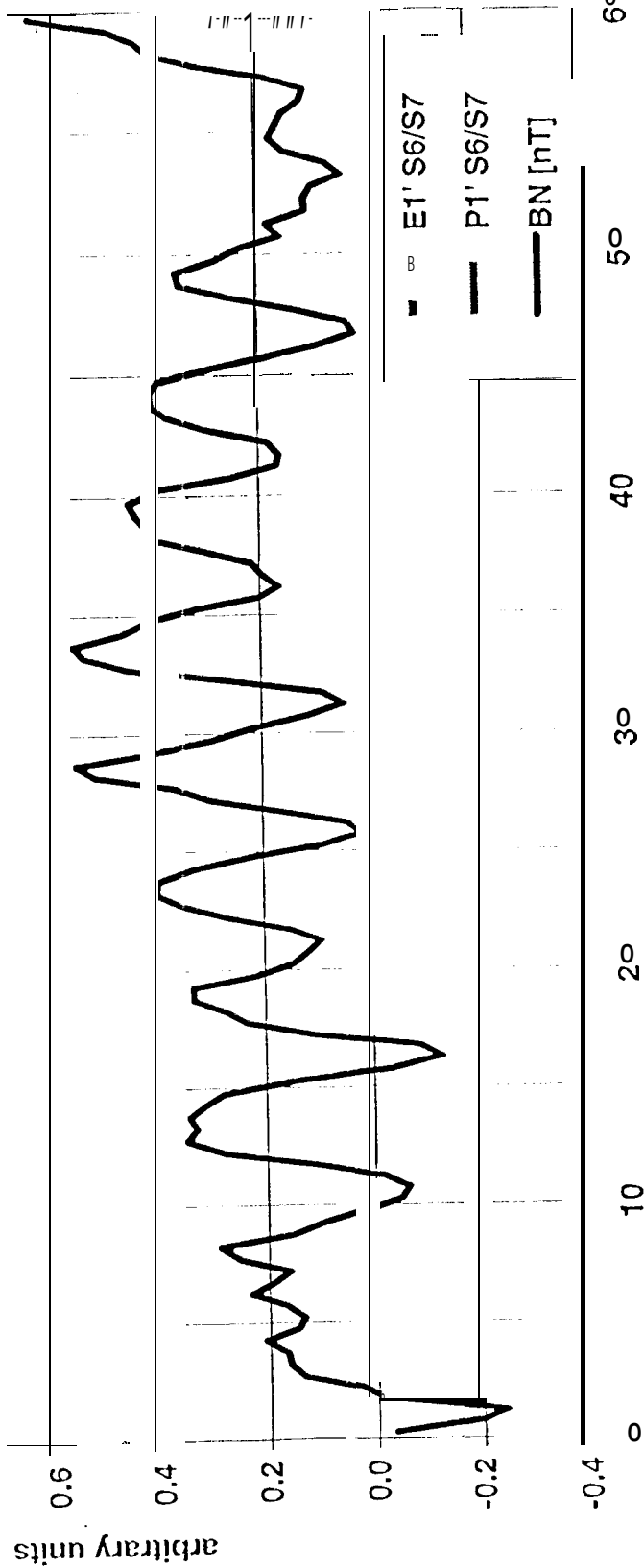
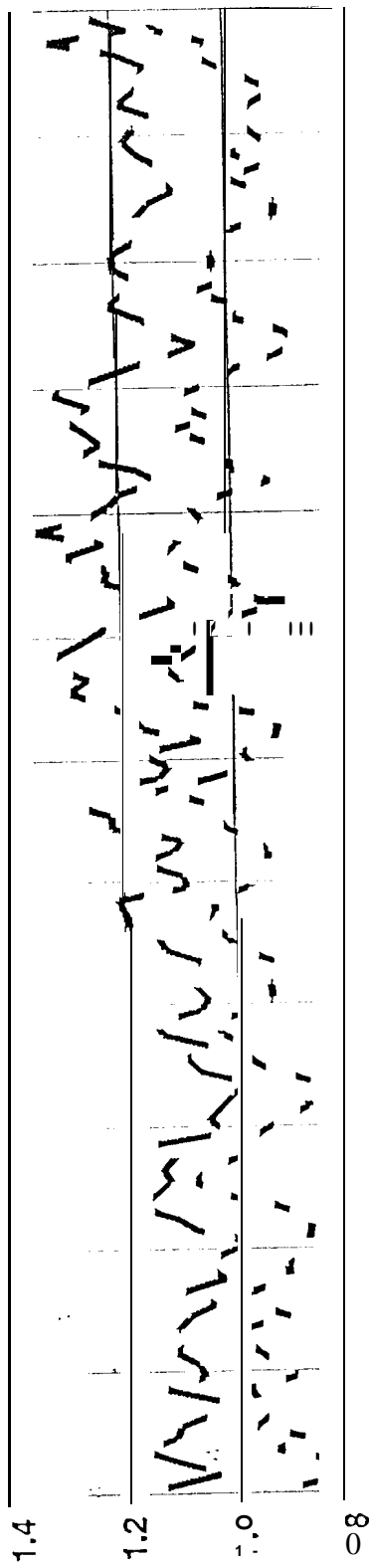
92 042 17:47:0.0
 92 042 17:48:0.0
 (58.8, 1.6)

92 042 17:48:0.0
 92 042 17:49:0.0
 (59.0, 0.1)

ELECTRONS

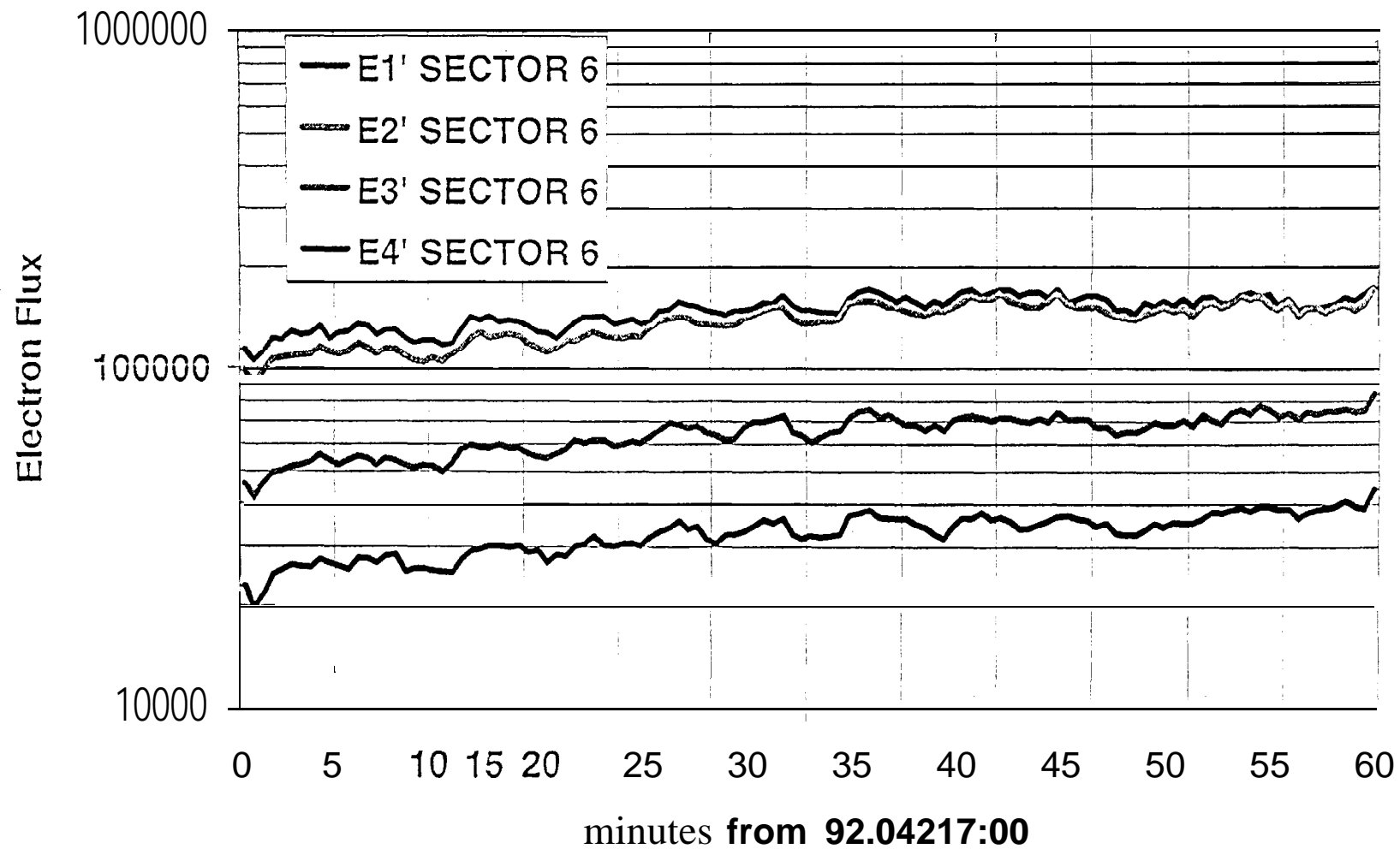
IONS

TIME →



minutes from 92.042.17:00

ULYSSES HI-SCALE LEFS60 EI '-E4' electrons (42-290 keV)



1987+16.10

ENERGY DENSITIES

